An All-Optical Ka-Band Microwave Long-Distance Dissemination System Based on an Optoelectronic Oscillator

Kaiyu Zhang, Shangyuan Li, Zhengyang Xie, and Zheng Zheng

***Abstract*—We proposed an all-optical Ka-band microwave long-distance dissemination system based on an optoelectronic oscillator (OEO). In this system, a single tone with high spectrum purity and low phase noise is excited by an injection-locked OEO, and distributed to the remote site through the fiber loop of the OEO at the same time. The second harmonic of the reference signal modulates the round-tripping optical signal at the local site, which achieves the phase conjugator at the optical domain. At the remote end, the phase-conjugated signal is photomixed with the OEO signal to eliminated the phase offset. The proposed scheme improves the phase noise of the high frequency signal received at the remote site and reduces the photoelectric conversion loss. We demonstrated the transmissions of a 36 GHz frequency-quadrupled RF signal along a 6 km optical fiber loop, and the frequency stability is 1.069 $\times$ 10^{-14}/1 s and 3.3 $\times$ 10^{-16}/1000 s. The single-sideband (SSB) phase noise of the received signal at the remote site is up to -130 dBc/Hz at 10 kHz offset frequency.**

***Index Terms*—Stable frequency dissemination, optoelectronic oscillator, passive phase compensation.**

I. Introduction

THE high-precision frequency transmission technique plays an important role in the infrastructure construction and cutting-edge scientific research fields, such as precise time-keeping, navigation and positioning, radar networking, detection of deep space, and precise measurement [1]–[3]. Compared with atmospheric channels and satellite links, optical fiber links have the advantages of low loss, high reliability, and anti-electromagnetic interference, which are suitable for the long-distance transmission of signals [4]. However, the length and refractive index of the optical fibers are susceptible to environmental temperature and mechanical vibration, which may cause phase fluctuations of the signal and deteriorate the frequency stability at the remote site [5].

Manuscript received 11 May 2022; revised 15 July 2022; accepted 30 July 2022. Date of publication 2 August 2022; date of current version 15 August 2022. This work was supported by the National Natural Science Foundation of China under Grants 61901026, 61690191, 61420106003, and 61621064. *(Corresponding author: Zhengyang Xie.)*

Kaiyu Zhang, Zhengyang Xie, and Zheng Zheng are with the Department of Electronic Engineering, Beihang University, Beijing 100191, China (e-mail: zkyvan@buaa.edu.cn; xiezy@buaa.edu.cn; zhengzheng@buaa.edu.cn).

Shangyuan Li is with the Beijing National Research Center for Information Science and Technology, Department of Electronic Engineering, Tsinghua University, Beijing 100084, China (e-mail: syli@mail.tsinghua.edu.cn).

Digital Object Identifier 10.1109/JPHOT.2022.3195935

In recent years, the phase-stable transmission of microwave signals based on phase compensation has been proposed and widely discussed, which can be classified into the active and passive compensation. For the active compensation scheme, the phase jitter is eliminated usually by performing phase detection and compensation algorithms on the signals to correct and offset the phase jitter [6]–[8]. However, the processing bandwidth is severely limited by the electrical compensation components. At the same time, additional thermal noise will also be induced, deteriorating the frequency stability of the system. For example, phase shifter and phase-locked loop (PLL) based compensation methods have achieved a long-term frequency stability of 10^{-17} at 10000 s averaging time for low-frequency RF only within 2.4 GHz [6], [7]. The passive compensation scheme usually uses a mixer and a frequency multiplier to perform a conjugate inversion on the phase offset of the received signals, and the phase jitter is thus eliminated by transmitting it back to the remote end. It not only overcomes the bandwidth limitation of electrical devices but also has a simple structure [9]–[11]. In 2017, the passive phase compensation for fiber-optic radio frequency transfer achieves the 10^{-16} level at 10000s averaging time over a 40 km point-to-point link [11]. However, the phase conjugation process requires RF non-linear devices, which will cause LO leakage and harmonic spurs. These frequency components will be superimposed on the phase noise spectrum and further deteriorate the frequency stability at the remote site.

In this paper, we propose and experimentally demonstrate an all-optical Ka-band microwave long-distance dissemination system based on an OEO. A local oscillator (LO) with an excellent phase noise performance is excited by the OEO and acts as a probe signal to sense the delay variation by distribution to the remote end through the OEO fiber loop [12], [13]. The reference microwave signal is injected into the OEO loop to suppress side modes and stabilize the single-mode oscillation [14], [15]. The OEO signal back to the local site is photomixed with the second harmonic of the reference signal to generate a phase-conjugated signal [16]. At the remote end, the backward phase-conjugated signal is photomixed with the probe signal to obtain a quadruple frequency signal, of which the phase is stabilized. A 36 GHz frequency-quadrupled RF signal is steadily disseminated along a 6 km fiber-optic loop link to a remote site with -130 dBc/Hz of the phase noise. The experimental result shows that the long-time stability is 3.3 $\times$ 10^{-16} at 1000 s averaging time. The

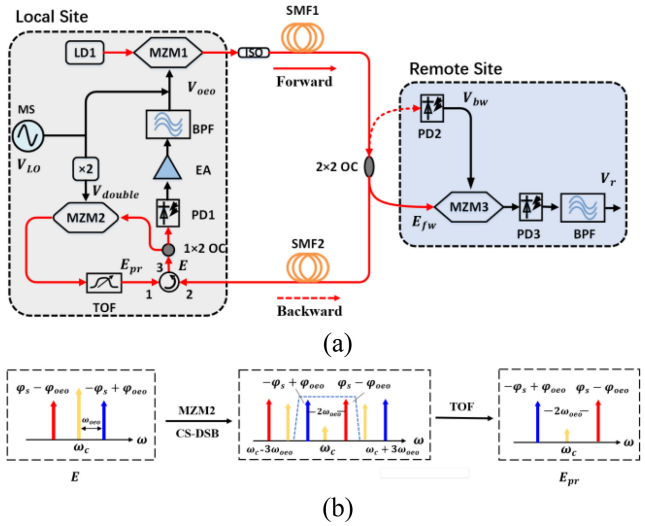

Fig. 1. (a) The schematic diagram of the proposed all-optical Ka-band microwave long-distance dissemination system based on an OEO. MS, microwave source; LD, laser diode; MZM, Mach-Zehnder modulator; TOF: tunable optical filter; PD: photodetector; EA: electric amplifier; OC: optical coupler; ISO: isolator; BPF: bandpass filter; SMF: single-mode fiber. (b) The spectrum of the photonic-microwave phase conjugation.

method of all-optical signal processing reduces the photoelectric conversion loss and avoids LO leakage and harmonic spurs caused by RF non-linear devices. Simultaneously, the proposed system utilizes a lower microwave frequency to disseminate stable mm-wave frequency, which alleviates the dependence on high-cost millimeter wave components.

II. System Architecture and Operation Principle

The schematic diagram of the all-optical Ka-band microwave long-distance dissemination system based on an OEO is illustrated in Fig. 1(a). The remote station is located at the junction of 4 km and 2 km single-mode fibers (SMF1 and SMF2), and the optical fiber loop also serves as the resonant cavity of the OEO. The OEO oscillation signal detects the phase delay of the optical fiber loop. At the local site, the OEO signal and the reference RF signal with doubled frequency are modulated together to the Mach-Zehnder modulator (MZM) for all-optical microwave phase conjugation. Then the phase-conjugated signal is transmitted in the reverse direction to the remote site to perform the all-optical mixing with the forward signal, which can eliminate the phase jitter caused by the optical fiber.

The optical section of the OEO is consist of a laser diode (LD1), a Mach-Zehnder modulator (MZM1), the fiber loop, and a photodetector (PD1). In the electrical section, the generated oscillation signal is amplified, and selected by the band-pass filter (BPF). We can express the oscillation signal as

$$V_{oeo} \propto \cos\left(\omega_{oeo}t + \varphi_{oeo} - \varphi_s\right), \tag{1}$$

where $\omega_{oeo} = 2\pi f_{oeo}$ is the oscillation frequency, φ_{oeo} and φ_s are the initial phase of the OEO and the phase offset introduced by the fiber loop. The reference LO signal is expressed as

$$V_{LO} \propto \cos\left(\omega_{LO}t + \varphi_{LO}\right), \tag{2}$$

where ω_{LO} is the angular frequency and φ_{LO} is the initial phase. As a multi-mode oscillation system, OEO allows multiple oscillation frequencies to exist at the same time, which will introduce interference signals during mixing and further deteriorate the stability of the system. Therefore, the system uses OEO with the injection-locked structure. The reference LO generated by the microwave source is coupled into the MZM1 to achieve the single-mode oscillation and suppress the side modes. The injection locking of the OEO depends on the injected power and the injected frequency difference of the injected signal [17]. The range of bandwidth that can achieve injection locking is represented by the locking bandwidth, which is

$$\Delta\omega_L = \omega_{oeo} - \omega_{LO} = \frac{\omega_{oeo}}{2Q}\frac{V_{LO}}{V_{oeo}}, \tag{3}$$

where Q is the quality factor of the OEO. It can be seen that the bandwidth of injection locking is proportional to the power of injected signal. Within the locking bandwidth, the phase noise of the frequency near the carrier is determined by the phase noise of the injected signal, while the phase noise of that far from the carrier is determined by the phase noise of the oscillator itself [18]. When the reference LO signal is locked by the OEO, its frequency is equal to that of the oscillation signal and the phase difference is constant, which is

$$\omega_{oeo} = \omega_{LO} \tag{4}$$

$$\varphi_{LO} - \varphi_{oeo} = const. \tag{5}$$

The remote station receives part of the forward transmission signal through the optical coupler (OC), which is expressed as

$$E_{fw} \propto \exp\left[j\omega_c\left(t - \tau_1\right)\right] \cdot \left\{\begin{array}{l} 1 + \exp\left[-j\left(\omega_{oeo}t - \varphi_1 + \varphi_{oeo}\right)\right] \\ + \exp\left[j\left(\omega_{oeo}t - \varphi_1 + \varphi_{oeo}\right)\right] \end{array}\right\}, \tag{6}$$

where τ_1 is the propagation delay introduced by single-mode fiber (SMF1) and $\varphi_1 = \omega_{oeo}\tau_1$ is the corresponding phase change of τ_1. And the signal transmitted back to the local site through the fiber optic loop is

$$E \propto \exp\left[j\omega_c\left(t - \tau_s\right)\right] \cdot \left\{\begin{array}{l} 1 + \exp\left[-j\left(\omega_{oeo}t - \varphi_s + \varphi_{oeo}\right)\right] \\ + \exp\left[j\left(\omega_{oeo}t - \varphi_s + \varphi_{oeo}\right)\right] \end{array}\right\}, \tag{7}$$

where $\tau_s = \tau_1 + \tau_2$ is the transmission delay of the fiber loop (SMF1+SMF2), which means φ_2 is the phase shift introduced by SMF2 and $\varphi_s = \varphi_1 + \varphi_2$ denotes the phase change of the round trip. At the local site, the frequency-doubled LO signal is expressed as

$$V_{double} \propto \cos\left(2\omega_{LO}t + 2\varphi_{LO}\right). \tag{8}$$

V_{double} is modulated into the upper arm of MZM2, which is operated at the null point for CS-DSB modulation. The spectrum evolution of the modulation procedure is shown in Fig. 1(b). The upper (blue) and lower (red) optical sidebands of the signal E carry the phase fluctuation $-\varphi_s$ and φ_s, respectively. Ignoring the effect of high-order optical sidebands (OSBs), the two first-order OSBs in the middle realize phase exchange after CS-DSB

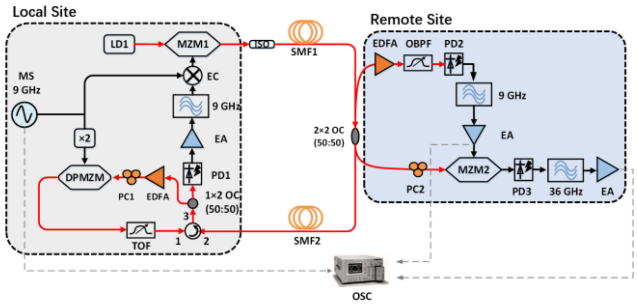

Fig. 2. Experimental setup of frequency dissemination system. MS, microwave source; LD, laser diode; PC: polarization controller; MZM, Mach-Zehnder modulator; EDFA: erbium-doped fiber amplifier; DPMZM, dual-parallel Mach-Zehnder modulator; EC: electric coupler; TOF: tunable optical filter; PD: photodetector; EA: electric amplifier; OC: optical coupler; ISO: isolator; BPF: bandpass filter; SMF: single-mode fiber; OSC: Oscilloscope.

modulation of MZM2. Then the TOF filters out the sidebands except for the two first-order OSBs, and the output signal is expressed as

$$E_{pr} \propto \exp\left[j\omega_c\left(t-\tau_s\right)\right] \cdot \left\{\begin{array}{l}\alpha+\exp\left[-j\left(\omega_{LO}t+\varphi_s-\varphi_{oeo}+2\varphi_{LO}\right)\right] \\ +\exp\left[j\left(\omega_{LO}t+\varphi_s-\varphi_{oeo}+2\varphi_{LO}\right)\right]\end{array}\right\}, \quad (9)$$

Where α is the carrier suppression ratio of MZM2. It represents the power ratio between the optical carrier and the first-order OSB. Hence, the photonic microwave phase conjugation is attained.

The phase-conjugated signal is backward transmitted to the remote site through the circulator and SMF2. After photodetection by PD2 and frequency selection by BPF, the phase-conjugated RF signal is

$$\begin{aligned} V_{bw} &\propto \cos\left(\omega_{LO}t+\varphi_s-\varphi_2+2\varphi_{LO}-\varphi_{oeo}\right) \\ &= \cos\left(\omega_{LO}t+\varphi_1+2\varphi_{LO}-\varphi_{oeo}\right). \end{aligned} \quad (10)$$

Note that, the propagation delay introduced by forward and backward transmission of signals on SMF2 is same because of the slow fiber-delay vibration [19]. The backward phase-conjugated signal V_{bw} modulates the forward transmission signal E_{fw} through MZM3. After PD3, the phase $-\varphi_1$ and φ_{oeo} of E_{fw} is counteracted by the phase φ_1 and $-\varphi_{oeo}$ of V_{bw}. Therefore, the signal obtained by the beat of second-order sideband is filtered out by a BPF and expressed as

$$V_r \propto \cos\left(4\omega_{LO}t+4\varphi_{LO}\right), \quad (11)$$

the frequency and phase of which are four times that of the reference LO signal V_{LO}. Meanwhile, the phase drift introduced by the fiber loop has been automatically counteracted.

III. Experiment and Discussion

To verify the performance of the proposed scheme, a proof-of-concept experiment was carried out based on Fig. 2. The local station and the remote station are connected by a 20-kmfiber loop link, consisting of 2 km and 4 km SMF jointed by a 50:50 OC. To further achieve the ultra-low phase noise, we used the G.655 non-zero dispersion-shifted single-mode fiber to replace

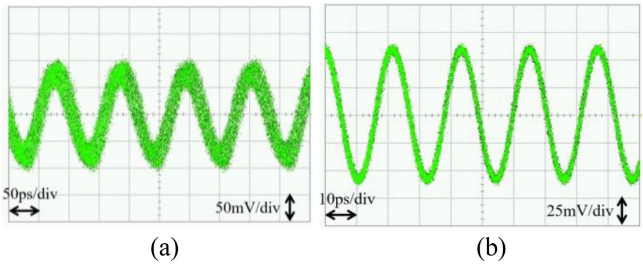

Fig. 3. Waveforms of the RF signal received at the remote site; (a) 9 GHz RF signal without compensation; (b) 36 GHz RF signal with compensation.

the G.652 single-mode fiber [20]. At the local site, a continuous laser (emcore, 1782A) is used to generate an optical carrier with the wavelength of 1547.92 nm and the power of 18 dBm. A 9 GHz reference RF signal is generated by the vector signal generator (KEYSIGHT, E8267D) locked with a rubidium clock. Then the RF signal is injected into the MZM1 together with the OEO loop signal to achieve injection locking. For MZM1, we used a 10 Gb/s intensity modulator which is biased at the linear operating point. A single-drive dual-parallel MZM (SD-DPMZM, Fujitsu FTM7961EX) is selected to attain a higher carrier suppression ratio in the part of all-optical microwave phase conjugation [21].

At the remote station, the optical signal transmitted backward is enhanced by an erbium-doped fiber amplifier (EDFA), and the input optical power of the PD2 is maintained at about 5 dBm. Both PD1, PD2 and PD3 are 40 Gb/s high-speed PDs (XPD2120R) with a bandwidth of 40 GHz. The amplified spontaneous emission (ASE) noise derived from the EDFA is suppressed by the optical bandpass filter (OBPF). The MZM2 of the remote station is a 40 Gb/s intensity modulator, which is biased at a quadrature point. In addition, we used two polarization controllers (PC1 and PC2) to control the polarization state and reduce polarization-dependent loss. A digital sampling oscilloscope (Agilent 86100C) triggered by the 9 GHz standard RF signal is utilized to record the waveforms and measure the timing delay variation.

To verify the compensation performance of the proposed scheme intuitively, we firstly measured the persistent waveform of the received signal under 1000 s of temperature drift. In the laboratory environment, the temperature may fluctuate about 1 °C. Fig. 3 shows the waveforms of the signal at the remote end without compensation and with the proposed microwave-photonic phase compensation respectively, which are V_{bw} and V_r in Fig. 1. It can be seen that without phase compensation, the 9 GHz RF signal V_{bw} exhibits large phase jitter under long-term temperature drift. In contrast, the phase shift of the 36 GHz signal V_r is significantly suppressed.

Fig. 4 shows the SSB phase noise of the free-running OEO and the 9 GHz LO injection signal. The phase noise of the free-running OEO is about −140 dBc/Hz at the 10 kHz offset, which is 20 dB lower than that with the reference signal. It means that the OEO can significantly improve the phase noise compared with the LO signal at the 10 kHz offset frequency. It can also be noticed that there is the peak at around 20∼30 kHz

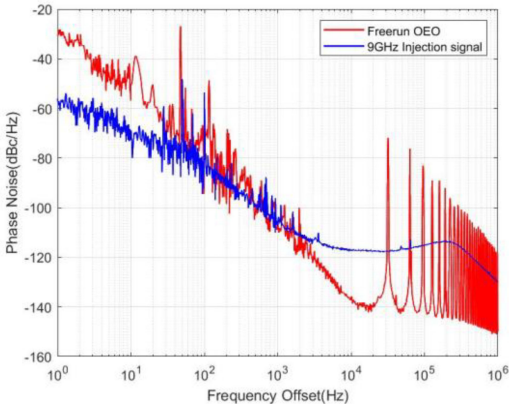

Fig. 4. Comparison of the phase noise spectra of the free-running OEO and the 9 GHz LO injection signal.

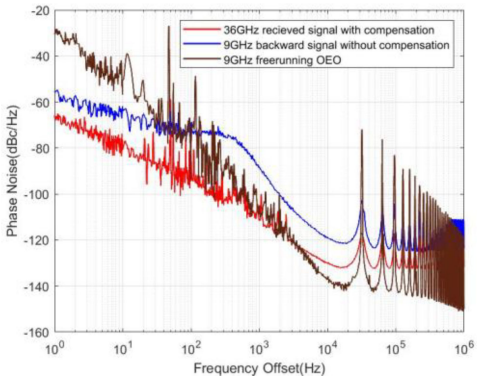

Fig. 5. Comparison of the phase noise spectra of the free-running OEO signal, 9 GHz backward signal without compensation and the 36 GHz received signal with microwave-photonic phase compensation.

offset frequency and its harmonics, which are the multimode oscillation of the free-running OEO. The frequency of cavity modes is related to the total delay of the OEO loop.

To compare the phase noise performance of the signal received at the remote site, Fig. 5 shows the SSB phase noise of the 9 GHz backward signal V_{bw} without compensation, the 36 GHz reference signal without compensation, and the 36 GHz received signal V_r with phase compensation. The phase noise of 9 GHz signal V_{bw} without compensation is about -120 dBc/Hz at 10 kHz offset. With the microwave-photonic phase compensation, the phase noise of the 36 GHz quadruple frequency signal at the remote site decreases to -130 dBc/Hz at 10 kHz offset. Meanwhile, the spurious modes of OEO deteriorate the phase noise at the high frequency offsets, which is reflected in the spectrum by the peaks at the cavity mode frequency from the central frequency [22]. The phase noise of signal with compensation is 50 dB lower at 30 kHz offset than that of the free-funning OEO signal. This represents that the system has a remarkable suppression on the side mode separated by about 30 kHz from the center frequency. It testified the effectiveness of the scheme.

We used overlapping Allan deviation (ADEV) to characterize the long-term frequency stability of this system at the 2 km$\sim$4

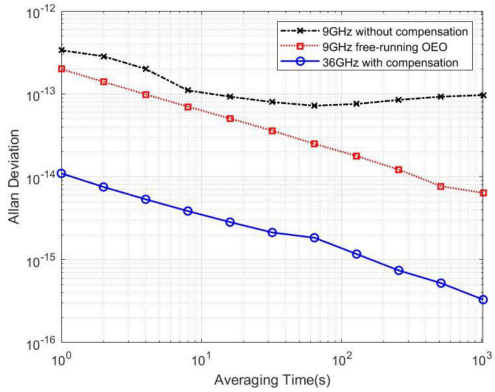

Fig. 6. The Allan deviation of the proposed frequency dissemination scheme.

km optical fiber loop. In Fig. 6, the ADEV of the 9 GHz free-running OEO signal, which is red line, is 2.0×10^{-13}/1 s and 6.3×10^{-15}/1000 s. And the ADEV of the 9 GHz RF signal V_{bw} without compensation is 3.4×10^{-13}/1s and 9.7×10^{-14}/1000 s, which is deteriorated due to the frequency random-walk noise brought by external factors and phase noise [23]. The blue line is the result of the 36 GHz signal with compensation. It can be seen that the ADEV is improved to 1.1×10^{-14} at 1s and 3.3×10^{-16} at 1000 s. According to the results, there are two orders of magnitude improvements of the frequency stability at 1000 s averaging time and the ADEV at 1 s averaging time is also promoted by nearly 20 times than that without compensation.

The system proposed a frequency transfer method over a single fiber with the same wavelength, which can maximize the symmetry of bidirectional transmission. The single optical wavelength can also avoid fluctuations of the group delay induced by temperature. However, it is necessary to consider the effect of backward Rayleigh scattering. Backward Rayleigh scattering noise is related to the power intensity of the input signal. It is calculated that the intensity of backward Rayleigh scattering noise caused by the optical signal input into the circulator is submerged by the noise floor. Besides, the EDFAs in Fig. 2 are all unidirectional amplifiers. Therefore, the system can effectively suppress the interference of backward Rayleigh scattering.

V. Conclusion

In summary, we propose and demonstrate an all-optical Ka-band microwave long-distance dissemination system based on an OEO. The low phase noise characteristic of OEO generates the RF signal with a high quality factor, and the long optical fiber of OEO is used as a method for LO distribution. Based on the traditional passive phase compensation, this scheme combines the all-optical signal processing with the advantages of high frequency, large bandwidth, and ultra-low phase noise of OEO to achieve the stable phase transmission of mm-wave signals. At the remote site, a 36 GHz quadruple frequency signal without phase jitter can be obtained, and the frequency stability of that is 1.1×10^{-14} and 3.3×10^{-16}. The SSB phase noise of the signal is up to –130 dBc/Hz at 10 kHz offset frequency. The

system proposed a ring topology for frequency quadrupling LO distribution, which reduces the requirements for mm-wave components. In addition, this scheme provides feasibility verification for fiber optic communication network based on high frequency carrier, such as 5G communication bearer network in Ka and millimeter-wave frequency bands [24].

REFERENCES

[1] J.-F. Cliché and B. Shillue, "Applications of control precision timing control for radioastronomy maintaining femtosecond synchronization in the atacama large millimeter array," *IEEE Control Syst. Mag.*, vol. 26, no. 1, pp. 19–26, Feb. 2006.

[2] A. W. Blain, "The ALMA telescope shows its true colours," *Nature*, vol. 495, no. 7441, pp. 324–325, Mar. 2013.

[3] M. Calhoun, S. Huang, and R. L. Tjoelker, "Stable photonic links for frequency and time transfer in the deep-space network and antenna arrays," *IEEE Proc.*, vol. 95, no. 10, pp. 1931–1946, Oct. 2007.

[4] J. Miao, B. Wang, Y. Bai, Y. B. Yuan, C. Gao, and L. J. Wang, "Portable microwave frequency dissemination in free space and implications on ground-to-satellite synchronization," *Rev. Sci. Instruments*, vol. 86, no. 5, May 2015, Art. no. 054704.

[5] M. Jiang et al., "Multi-access RF frequency dissemination based on round-trip three-wavelength optical compensation technique over fiber-optic link," *IEEE Photon. J.*, vol. 11, no. 3, Jun. 2019, Art. no. 7202808.

[6] R. Wu, J. Lin, T. Jiang, C. Liu, and S. Yu, "Stable radio frequency transfer over fiber based on microwave photonic phase shifter," *Opt. Exp.*, vol. 27, no. 26, pp. 38109–38115, Dec. 2019.

[7] S. Zhou et al., "Stable RF transmission in dynamic phase correction with Rayleigh backscattering noise suppression," *Opt. Fiber Technol.*, vol. 56, May 2020, Art. no. 102165.

[8] J. Zhang, G. Wu, T. Lin, and J. Chen, "Fiber-optic radio frequency transfer based on active phase noise compensation using a carrier suppressed double-sideband signal," *Opt. Lett.*, vol. 42, no. 23, pp. 5042–5045, Dec. 2017.

[9] Y. Chen et al., "Stable radio frequency transfer over free space by passive phase correction," *IEEE Photon. J.*, vol. 11, no. 6, Dec. 2019, Art. no. 5503308.

[10] C. Hu, B. Luo, W. Bai, W. Pan, L. Yan, and X. Zou, "Stable radio frequency transmission of single optical source over fiber based on passive phase compensation," *IEEE Photon. J.*, vol. 13, no. 1, Feb. 2021, Art. no. 7200607.

[11] T. Lin, G. Wu, H. Li, G. Wang, and J. Chen, "Passive phase noise compensation for fiber-optic radio frequency transfer with a non-synchronized source," *Chin. Opt. Lett.*, vol. 16, no. 10, pp. 9–12, 2018.

[12] X. S. Yao and L. Maleki, "Optoelectronic microwave oscillator," *J. Opt. Soc. Amer. B*, vol. 13, pp. 1725–1735, 1996.

[13] S. Li, K. Zhang, H. Wang, and Z. Xie, "Stable microwave LO distribution via a phase-locked OEO assisted by passive compensation," *Opt. Commun.*, vol. 507, Mar. 2022, Art. no. 127625.

[14] O. Okusaga et al., "Spurious mode reduction in dual injection-locked optoelectronic oscillators," *Opt. Exp.*, vol. 19, no. 7, pp. 5839–5854, Mar. 2011.

[15] Z. Fan, Q. Qiu, J. Su, and T. Zhang, "Tunable low-drift spurious-free optoelectronic oscillator based on injection-locking and time-delay compensation," *Opt. Lett.*, vol. 44, no. 3, pp. 534–538, Feb. 2019.

[16] H. Wang, X. Xue, S. Li, and X. Zheng, "All-optical arbitrary-point stable quadruple frequency dissemination with photonic microwave phase conjugation," *IEEE Photon. J.*, vol. 10, no. 4, Aug. 2018, Art. no. 5501508.

[17] B. Razavi, "A study of injection locking and pulling in oscillators," *IEEE J. Solid-State Circuits*, vol. 39, no. 9, pp. 1415–1424, Sep. 2004.

[18] A. Banerjee, L. A. D. de Britto, and G. M. Pacheco, "A theoretical and experimental study of injection-locking and injection-pulling for optoelectronic oscillators under radio frequency signal injection," *J. Lightw. Technol.*, vol. 38, no. 6, pp. 1210–1220, Mar. 2020.

[19] W. Li, W. Wang, W. Sun, W. Wang, and N. Zhu, "Stable radio-frequency phase distribution over optical fiber by phase-drift auto-cancellation," *Opt. Lett.*, vol. 39, pp. 4294–4296, 2014.

[20] K. Volyanskiy, Y. K. Chembo, L. Larger, and E. Rubiola, "Contribution of laser frequency and power fluctuations to the microwave phase noise of optoelectronic oscillators," *J. Lightw. Technol.*, vol. 28, no. 18, pp. 2730–2735, Sep. 2010.

[21] S. Li, X. Zheng, H. Zhang, and B. Zhou, "Compensation of dispersion-induced power fading for highly linear radio-over-fiber link using carrier phase-shifted double sideband modulation," *Opt. Lett.*, vol. 36, pp. 546–548, 2011.

[22] D. Eliyahu and L. Maleki, "Low phase noise and spurious level in multi-loop opto-electronic oscillators," in *Proc. IEEE Int. Freq. Control Symp. PDA Exhib., 17th Eur. Freq. Time Forum*, 2003, pp. 405–410.

[23] E. Rubiola, *Phase Noise and Frequency Stability in Oscillators*. Cambridge, U.K.: Cambridge Univ. Press, 2008.

[24] M. Shafi et al., "5G: A tutorial overview of standards trials challenges deployment and practice," *IEEE J. Sel. Areas Commun.*, vol. 35, no. 6, pp. 1201–1221, Jun. 2017.